Published in final edited form as:
Neuroimage. 2012 July 16; 61(4): 1226–1234. doi:10.1016/j.neuroimage.2012.03.010.

Disconnectivity of the Cortical Ocular Motor Control Network in Autism Spectrum Disorders

Tal Kenet[a,d,‡], **Elena V. Orekhova**[d,1,*], **Hari Bharadwaj**[a,d,2,*], **Nandita R. Shetty**[a,d], **Emily Israeli**[a,d], **Adrian K.C. Lee**[b,d,3], **Yigal Agam**[b,d], **Robert M. Joseph**[e], **Matti S. Hämäläinen**[c,d], and **Dara S. Manoach**[b,d]

Dara S. Manoach: dara@nmr.mgh.harvard.edu

[a]Department of Neurology, Massachusetts General Hospital, Boston, MA 02114, USA

[b]Department of Psychiatry, Massachusetts General Hospital, Boston, MA 02114, USA

[c]Department of Radiology, Massachusetts General Hospital, Boston, MA 02114, USA

[d]Athinoula A. Martinos Center for Biomedical Imaging, 149 13th St., Charlestown, MA 02129, USA

[e]Department of Anatomy and Neurobiology, Boston University School of Medicine, 72 East Concord St., Boston, MA, USA

Abstract

Response inhibition, or the suppression of prepotent but contextually inappropriate behaviors, is essential to adaptive, flexible responding. Individuals with autism spectrum disorders (ASD) consistently show deficient response inhibition during antisaccades. In our prior functional MRI study, impaired antisaccade performance was accompanied by reduced functional connectivity between the frontal eye field (FEF) and dorsal anterior cingulate cortex (dACC), regions critical to volitional ocular motor control. Here we employed magnetoencephalography (MEG) to examine the spectral characteristics of this reduced connectivity. We focused on coherence between FEF and dACC during the preparatory period of antisaccade and prosaccade trials, which occurs after the presentation of the task cue and before the imperative stimulus. We found significant group differences in alpha band mediated coherence. Specifically, neurotypical participants showed significant alpha band coherence between the right inferior FEF and right dACC and between the left superior FEF and bilateral dACC across antisaccade, prosaccade, and fixation conditions. Relative to the neurotypical group, ASD participants showed reduced coherence between these regions in all three conditions. Moreover, while neurotypical participants showed increased coherence between the right inferior FEF and the right dACC in preparation for an antisaccade compared to a prosaccade or fixation, ASD participants failed to show a similar increase in preparation for the more demanding antisaccade. These findings demonstrate reduced long-range functional connectivity in ASD, specifically in the alpha band. The failure in the ASD group to

[‡]Corresponding author, Massachusetts General Hospital, 149 13th St., CNY-10.023, Charlestown, MA 02129. tal@nmr.mgh.harvard.edu, Ph: 617-643-6732, Fax: 617-643-7792.
[*]Equal contribution
[1]Present address: Institute of Neuroscience and Physiology, University of Gothenburg, Box 432, SE-405 30, Göteborg, Sweden
[2]Present address: Department of Biomedical Engineering, Boston University, 44 Cummington St., Boston, MA
[3]Present address: Institute for Learning & Brain Sciences, University of Washington, 1715 Columbia Road N., Seattle, WA 98195

increase alpha band coherence with increasing task demand may reflect deficient top-down recruitment of additional neural resources in preparation to perform a difficult task.

Keywords

Autism; ASD; Connectivity; Alpha Synchrony; MEG

1. Introduction

Autism spectrum disorders (ASD) are defined by impaired social interactions, impaired communication, and repetitive and restricted behaviors. Individuals with ASD also consistently show deficient response inhibition, which is accompanied by reduced functional connectivity in cognitive control networks in functional MRI (fMRI) studies (Agam et al., 2010; Kana et al., 2007). In particular, ASD is characterized by higher error rates on antisaccade tasks (Goldberg et al., 2002; Manoach et al., 2004; Minshew et al., 1999; Mosconi et al., 2009; Thakkar et al., 2008), which requires a gaze away from a suddenly appearing visual stimulus. Errors occur when participants fail to inhibit the prepotent response of looking towards the stimulus (i.e., a prosaccade). In our prior fMRI study, impaired antisaccade performance in ASD was accompanied by reduced functional connectivity between the frontal eye field (FEF) and the dorsal anterior cingulate cortex (dACC), which are anatomical components of a network involved in volitional ocular motor control (Agam et al., 2010). In addition, unlike neurotypical (NT) controls who showed increased activation in the FEF and dACC for antisaccades than for prosaccades, ASD participants failed to modulate activation levels in accordance with task demands. These findings are consistent with evidence that ASD is a disorder of connectivity (Just et al., 2007; Kleinhans et al., 2008; Koshino et al., 2008; Mostofsky et al., 2009) in which alterations in white matter integrity and reduced coordination of activity across brain regions give rise to the core diagnostic features and to characteristic cognitive deficits (Belmonte et al., 2004; Minshew and Williams, 2007).

The goal of the present study was to identify the spectral basis of the reduced functional connectivity and lack of task-dependent modulation of activity in the dACC and FEF that we previously observed in ASD (Agam et al., 2010). Since oscillations of different frequencies appear to have distinct mechanisms and roles in cognitive function (Uhlhaas and Singer, 2006; Uhlhaas et al., 2008; Uhlhaas et al., 2010), identifying the spectral signature of reduced connectivity between specific regions during deficient response inhibition in ASD may illuminate the neural bases of this deficiency. We used magnetoencephalography (MEG), which has excellent temporal and good cortical spatial resolution, during performance of the same antisaccade task used in the previous study (Fig. 1) (Agam et al., 2010) in a subset of the participants. Based on our fMRI findings, we hypothesized that FEF-dACC functional connectivity would be reduced in ASD, and that only NT participants would increase coherence between the FEF and the dACC in preparation for the more demanding antisaccade task. We further hypothesized that reduced connectivity in the ASD group would be mediated by reduced coherence in the alpha band, since alpha synchrony dominates visuospatial attention (Capotosto et al., 2009) and prior EEG (Coben et al., 2008; Murias et al., 2007) and MEG (Tsiaras et al., 2011) studies have found reduced alpha band coherence in ASD during resting state.

In the present study, the superior temporal resolution of MEG allowed us to limit our analyses to the preparatory period of saccadic trials, which occurs after the presentation of the task cue and before the imperative stimulus. The preparatory period emphasizes the cognitive aspects of task preparation since the task is known from the cue but the

appropriate motor action cannot be planned until the stimulus indicates the required direction. Importantly, preparatory activity in the FEF and other regions in the network for volitional ocular motor control differs for antisaccades versus prosaccades (Brown et al., 2007), and predicts the timing of saccadic responses in both human neuroimaging and monkey neurophysiology studies (Connolly et al., 2005; Connolly et al., 2002; Hamm et al., 2010; Nagel et al., 2008). We further limited the present study to correct trials because activation patterns for correct and error trials differ during the preparatory period (Everling and Munoz, 2000; Ford et al., 2005; McDowell et al., 2008). Finally, we chose to focus on cortical coherence with the FEF, since it is the key cortical region involved in generating volitional saccades (Pierrot-Deseilligny et al., 1995).

2. Methods

2.1. Participants

Eleven adults with ASD (9 males, 2 females, mean age 27.5 +/− 10.3 years) and 11 NT control participants (9 males, 2 females, mean age 29.5 +/− 9.8 years) were recruited by poster and website advertisements (see Table 1 for demographic data). Participants with ASD were diagnosed by an experienced clinician on the basis of current presentation and developmental history as determined by medical record review and clinical interview. ASD diagnoses were confirmed using the Autism Diagnostic Interview-Revised (ADI-R, Rutter, 2003) and the Autism Diagnostic Observation Schedule Module 4 (Lord, 1999) administered by experienced research personnel with established inter-rater reliability. Potential participants meeting DSM-IV criteria for co-morbid psychiatric conditions or with known autism-related medical conditions (e.g., Fragile-X syndrome, tuberous sclerosis) were excluded. Four ASD participants were taking the following medications: fluoxetine and lithium; bupropion and clonazepam; citalopram; and sertraline and methylphenidate. NT participants were screened to exclude a history of autism or any other neurological or psychiatric condition (SCID-Nonpatient edition, First, 2002). All participants were screened to exclude substance abuse or dependence within the preceding six months, as well as any independent condition that might affect brain function. One ASD participant who was included in the sensor space analysis was excluded from the cortical space analysis because of invalid head localization data. ASD and control groups were matched on age, sex, handedness as measured by a laterality score on the modified Edinburgh Handedness Inventory (Oldfield, 1971; White, 1976), parental socioeconomic status on the Hollingshead Index (Hollingshead, 1965), years of education, and estimated verbal IQ based on a test of single word reading (American National Adult Reading Test, Blair, 1989). The study was approved by the Partners Human Research Committee at Massachusetts General Hospital. All participants gave written informed consent after the experimental procedures had been fully explained.

2.2. Saccadic Paradigm

The task was explained prior to the MEG session, and participants practiced until their performance indicated that they understood the directions and were comfortable with the task. Participants were instructed not to blink until after generating the saccade, and to respond as quickly and accurately as possible. They were told that they would receive a 5-cent bonus for each correct response in addition to a base rate of pay. This incentive was intended to enhance motivation and attention during a potentially boring cognitive task in order to elicit optimal performance. No immediate feedback regarding performance was provided and the bonus was added to the remuneration check that was sent by mail following study completion. Saccadic task stimuli were generated using a Vision Shell programming platform (www.visionshell.com) and presented with a Digital Light Processing (DLP) InFocus 350 projector through an opening in the wall, onto a back-

projection screen placed 102 cm in front of the participant inside the magnetically shielded MEG suite. Each participant performed eight runs of the saccadic task with short breaks between runs. Figure 1 provides the task details. Each run lasted 5 min 22 s and consisted of a sequence of randomly interleaved prosaccade (PS), antisaccade (AS), and fixation (FIX) trials. The saccadic trials were balanced for rightward and leftward movements and lasted 4 s. FIX trials lasted 2, 4, or 6 s and required participants to maintain a steady gaze at the center of a screen display that was identical to and continuous with the last second of the previous saccadic trial. The total experiment lasted approximately one hour and generated a total of 278 PS, 285 AS, and 107 FIX trials.

2.3. Scoring of Eye Movement Data

Eye movements were recorded concurrently with MEG using two pairs of bipolar electro-oculogram (EOG) electrodes. The EOG data were scored in MATLAB using a partially automated program that determined the directional accuracy of each saccade with respect to the required response and its latency from target onset. Saccades were identified as horizontal eye movements with velocities exceeding 46.9 deg/s. The onset of a saccade was defined as the point at which the velocity of the eye first exceeded 31.3 deg/s. For saccade trials, only epochs with saccades in the desired direction (i.e., correct trials) with latencies between 130 and 800 ms were included for analysis. The cutoff of 130 ms excluded anticipatory saccades, which are not true responses to the appearance of the visual target (Doricchi et al., 1997; Fischer and Breitmeyer, 1987; Straube et al., 1999). We also excluded saccade trials if a saccade or eye blink (defined as vertical peak-to-peak EOG amplitude exceeding 200 μV) occurred during the baseline period (200 ms prior to cue onset) or the cue-stimulus interval (Fig. 1a, 0–2000 ms). For FIX, only trials without blinks or saccades were included and data from the following time windows were analyzed: 1000–2000 ms (available on all fixation trials), 3000–4000 ms (available from the 4 s fixation trials) and 5000–6000 ms (available from the 6 s fixation trials).

2.4. Structural MRI Acquisition

For source localization and spatial normalization, two T1-weighted high-resolution structural images were acquired during a separate session using a 3.0 T Siemens (Erlangen, Germany) Trio whole body high-speed imaging device equipped for echo planar imaging (EPI). We used a 3D magnetization-prepared rapid gradient echo (MPRAGE) sequence (repetition time (TR), 2530 ms; echo spacing, 7.25 ms; echo time (TE), 3 ms; flip angle 7°; voxel size, 1.3 × 1.3 × 1 mm). A 3D structural image was created for each participant by averaging the two MPRAGE scans after correcting for motion.

2.5 MEG Data Acquisition

MEG data were acquired inside a magnetically shielded room (IMEDCO, Hagendorf, Switzerland) using a dc-SQUID Neuromag™ Vector View system (Elekta-Neuromag, Helsinki, Finland) comprising a helmet-shaped array of 306 sensors, arranged in triplets of two orthogonal planar gradiometers and a magnetometer. The signal was filtered to a 0.1–200 Hz bandpass and sampled at 600 Hz. The position and orientation of the head with respect to the MEG sensor array were determined by four Head Position Indicator (HPI) coils. To allow registration of MEG and MRI data, the locations of three fiduciary points (nasion and auricular points) that define a head-based coordinate system, a set of points from the head surface, and the sites of the four HPI coils were digitized using a 3 Space Fastrak digitizer (Polhemus, Colchester, VT, USA) integrated with the Vectorview system.

2.6 Postprocessing of MEG Data

Spatial filtering was performed on the data using the Signal Space Separation (SSS) method (Taulu et al., 2004; Taulu and Simola, 2006). This step suppresses interference signals generated outside the brain. The SSS method reduces the dimensionality of the data from 306 components to 64 components. Independent Component Analysis (ICA) was then implemented on the magnetometers and gradiometers separately using the EEGlab suite to decompose the data into 64 statistically independent components (Delorme and Makeig, 2004). The heartbeat component was identified and removed, leaving 63 independent components. The final preprocessing of sensor data involved automated rejection of trials based on amplitude criteria. Epochs were rejected if the peak-to-peak peak value over the epoch exceeded 1000 fT and 3000 fT/cm in magnetometer and planar gradiometer channels, respectively.

2.7 Coherence Analysis

We analyzed coherence in the 1000 ms immediately preceding the imperative stimulus (indicated by the bold line in Fig. 1c) for correctly executed saccadic trials only. Activity during this period reflects general task preparation but not the planning of the actual saccadic response since the required direction of the eye movement was not known until the stimulus appeared. To compute the coherence between channels, we first used the MATLAB fast Fourier transform algorithm to compute the Fourier coefficient for each channel, in 1 Hz steps. We then calculated coherence between any two sensors x and y (C_{xy}) in each frequency band by normalizing the squared cross-spectral density of the time series from these two sensors (G_{xy}) by the power spectral density of the time series from each of these sensors (G_{xx} and G_{yy}):

$$C_{xy} = \frac{|G_{xy}|^2}{G_{xx} G_{yy}}$$

This yielded a value between 0 and 1, where a value of 1 means the phase between the two channels was identical for all epochs, and a value of 0 means the phase in one channel was random relative to the other channel across epochs. Coherence values were then averaged within each of the following six frequency band Delta (0–4 Hz), Theta (4–8 Hz), Alpha (8–12 Hz), Beta (12–30 Hz), Gamma1 (30–80 Hz) and Gamma2 (80–100Hz), to obtain a mean coherence value for each band. Since the estimate of coherence is biased by the number of epochs (Bokil et al., 2007), 95 randomly selected epochs per condition per subject were used for group analyses. This number was determined by the smallest number of usable trials available for any one participant (see Postprocessing of MEG Data, above). The average number of usable trials per participant was not significantly different between groups or across conditions.

2.7.1 Sensor Space Coherence Analysis—To complement our source space analysis, and to be comparable to prior studies of coherence in ASD, we first conducted a coherence analysis in the sensor space. We used the planar gradiometers to analyze coherence in sensor space. Coherence was calculated between every pair of gradiometers, at 102 sensor locations, resulting in 5,151 pairs. Since each sensor location has two orthogonal gradiometers, all four coherence values (2 × 2) were computed for each pair of sensor locations, and the maximum coherence value was used for each pair. The mean of the coherence values over each band was used for group analysis. We used the standard Fisher transform to make the coherence values normally distributed. We then followed a permutations procedure, similar to the one described in Murias et al. (Murias et al., 2007), to determine whether coherence in any sensor pair was different across groups. Specifically,

for each sensor pair, we used 1000 permutations across participants to determine whether coherence values for that sensor pair differed significantly by group.

2.7.2 Source Estimation—The geometry of each participant's cortical surface was reconstructed from the 3D structural MRI data using FreeSurfer software (http://surfer.nmr.mgh.harvard.edu). The cortical surface was decimated to a grid of 4098 dipoles per hemisphere, corresponding to a spacing of approximately 5 mm between adjacent source locations on the cortical surface. The MEG forward solution was computed using a single-compartment boundary-element model (BEM) assuming the shape of the intracranial space (Hämäläinen and Sarvas, 1987). The watershed algorithm was used to generate the inner skull surface triangulations from the T1-weighted MR images of each participant. Assuming head movements occurred only between runs and to compensate for these movements, the forward solutions for each run were computed and averaged (Uutela et al., 2001). The cortical current distribution was estimated using minimum-norm estimate (MNE) software (http://www.martinos.org/martinos/userInfo/data/sofMNE.php) and assuming the orientation of the source to be fixed perpendicular to the cortical mesh. The noise-covariance matrix used to calculate the inverse operator was estimated from data collected without a subject present. To reduce the bias of the MNEs towards superficial currents, we used depth weighting, i.e. adjusted the source covariance matrix to favor deep source locations (Lin et al., 2006).

2.7.3 Inter-Subject Cortical Surface Registration for Group Analysis—Each participant's inflated cortical surface was registered to an average cortical representation by optimally aligning individual sulcal-gyral patterns (Fischl et al., 1999b). We employed a surface-based registration technique based on folding patterns because it provides more accurate inter-subject alignment of cortical regions than volume-based approaches (Fischl et al., 1999b; Van Essen and Dierker, 2007).

2.7.4 Seed Region Definition for Cortical Space Coherence Analysis—Based on our *a priori* hypotheses, we limited our analyses to examining coherence between the FEF and the rest of the vertices in the cortex. We generated four FEF seed regions – the inferior and superior sections of the right and left FEF (FEFi-R, FEFi-L, FEFs-R, and FEFs-L respectively). Seed region definitions were based on both anatomical and functional constraints. The FEF is located in and around the precentral sulcus and gyrus (Koyama et al., 2004; Paus, 1996) with distinct regions in the superior and inferior portions (Luna et al., 1998; Simo et al., 2005). Since MEG is best able to detect tangential sources (i.e., those in sulci rather than gyri on the lateral surface) we used the superior and inferior precentral sulci from the FreeSurfer Average7 brain parcellations as the anatomical constraint for our ROIs (Lee et al., 2011; Moon et al., 2007). Within these anatomical boundaries we defined our functionally constrained seed regions by selecting vertices that were active during the preparatory period in the contrast of all saccades versus fixation at a threshold of $p<.05$ at any time point in either group for activity computed every 20 ms. The vertices were smoothed to generate contiguous labels, and the labels generated for each group were then merged.

2.7.4 Seed Region Time Course—We averaged across vertices within each of the four seed regions to compute their representative time courses. To avoid signal cancellation, the averaging took into account the polarity mismatches that occur because of MNE estimate spreading across sources whose orientations were not aligned. This was accomplished by inverting the polarity of the signals of those sources that were oriented at an obtuse angle (> 90°) with respect to a reference direction.

2.7.5 Source Space Coherence Analysis—Coherence values were calculated between the seed region time course and the time course at each of the 8,196 cortical sources (i.e., vertices), for each group, for each of the three trial types. To determine which sources showed significant coherence values, we applied the Fischer transform to normalize the distribution. We then performed a paired t-test against Fischer transformed coherence values computed from MEG recordings without a participant (empty-room) that were processed and inverted to source space using the same methods as were applied to the participant data (Fig. 2). This empty-room comparison suppresses artifactual coherence arising from the point spread of the MNE (Ghuman et al., 2011). After the empty-room correction, the expected mean coherence of the data in the absence of any real coherence is zero. Thus, any coherence values significantly greater than zero are interpreted to reflect true coherence. Finally, effects of group and condition were assessed using a repeated measures ANOVA. A False Discovery Rate (FDR) (Benjamini and Hochberg, 1995) of $q<.1$ was used to correct for multiple comparisons across all vertices. The $q<.1$ threshold was chosen based on current mathematical analyses and practices in the field (Efron, 2007; Genovese et al., 2002; Rutter et al., 2009). The assignment of vertices showing significant correlation with the FEF seeds to particular cortical regions was based on automatically generated FreeSurfer labels (Dale et al., 1999; Fischl et al., 1999a).

2.7.6 Averaging Coherence Values in the dACC—To compute the mean coherence values in the right and left dACC labels, we averaged the coherence values across all vertices of the dACC, per hemisphere. Thus, significant as well as non-significant coherence values within the dACC were averaged together to obtain, for each participant, the mean coherence value between the FEF and the dACC, which was then used for comparisons across groups and conditions.

3. Results

3.1. Behavioral Results

We excluded one NT control from the error analysis based on an error rate that was 3.75 standard deviations greater than the group mean. ASD participants did not significantly differ in errors from NT controls ($p = .12$) and this was true regardless of task (Group × Task, $p = 0.15$). Although ASD participants made almost twice as many antisaccade errors (20 ±14%) as controls (11 ±10 %) this difference did not reach significance ($p = .12$). The groups had a similar rate of prosaccade errors (ASD: 5 ±4 %; NT: 4 ±3 %; $p = .37$). There were no significant group differences in response time on correct trials ($p=.25$) regardless of task (Group × Task, $p=.40$; antisaccade: ASD 263 ±31, NT 287 ±37, $p = .13$; prosaccade: ASD 222 ±47; HC 237 ±39; $p = .44$).

3.2. Sensor-Space Coherence Differences

Sensor-space coherence was analyzed for each condition in all frequency bands and compared across groups. For each condition, about 30% of all sensor pairs showed reduced alpha band coherence in ASD ($p<.05$ uncorrected, supplementary Fig. S1), while only about 5% of sensor pairs, as expected by chance, showed differences in the other frequency bands. The distances between sensor pairs with reduced coherence in the ASD group were distributed approximately uniformly, indicating that field spread was not a confounding factor. Since we found no significant power differences between the groups in any condition, in any of the sensor locations, the observed coherence differences could not be attributed to variations in signal-to-noise ratio.

3.3. Cortical Coherence

Given the role of alpha coherence in visuospatial attention, prior findings of reduced alpha band coherence in ASD, and the findings of our sensor-space analyses, we first examined alpha band coherence in our FEF and dACC ROIs. We computed the coherence between each of the four FEF seed regions, and all other vertices in the cortex in all three conditions. We found that the NT group showed significant coherence ($q<.1$) between the FEFiR seed and vertices in the ipsilateral FEFsR, dACC, and the dorsolateral prefrontal cortex (DLPFC) (Fig. 2a,c). The NT group also showed significant coherence between the FEFsL seed and the dACC bilaterally. The FEFiL and FEFsR seeds were not significantly coherent with any other cortical regions. The same pairs of regions showed significant coherence in the ASD group (Fig. 2b,d). In both groups, only the FEFiR and FEFsL showed significant coherence with other cortical regions. Therefore, we limited further examination of group differences in coherence to these two seed regions. Again, we found no significant power differences between the groups in any condition, in any of the ROIs. Therefore, the observed coherence differences could not be attributed to variations in signal-to-noise ratio.

3.4. Group and Condition Differences in Coherence with the FEFiR Seed

Compared to the NT group, the ASD group showed significantly reduced coherence between the FEFiR seed and the right dACC across all three conditions. Importantly, only the NT group showed significant modulation of coherence based on task demands. Specifically, while the NT group showed increased coherence between these regions for AS relative to PS or FIX conditions, the ASD group failed to increase coherence for the AS condition and differed significantly from the NT group in this regard. Figure 3a shows the mean coherence between the FEFiR and the right dACC, averaged across all the vertices in the right dACC, per group, per condition. A repeated measures ANOVA in cortical space confirmed this result, demonstrating a group by condition interaction in the coherence between the FEFiR and the ipsilateral dACC ($F(2,38) > 11$, $p<1.7e-4$, $q<.1$). This result reflected both the general reduced coherence in ASD and the ASD group's lack of condition-driven modulation of coherence. Figure 3b shows the vertices that had significant group by condition interactions when the FEFiR seed was used to compute coherence. Consistent with the sensor-space results, we confirmed using source space analysis that none of the other frequency bands (i.e., Delta, Theta, Beta, Gamma1 and Gamma2) showed significant group differences in coherence between these regions in any of the three conditions.

3.5. Group Differences in Coherence with the FEFsL Seed

Coherence between the FEFsL and bilateral dACC did not differ by condition in either group, but was significantly lower in the ASD group relative to the NT group in all conditions. Figure 4 depicts the mean unbiased coherence between the FEFsL and all vertices of the left dACC (Fig. 4a) and right dACC (Fig. 4b), after empty room correction. Again, no other frequency band showed significant group differences in coherence between these regions in any of the three conditions.

4. Discussion

This is the first study to use source space analysis of MEG data to specify the spectral and spatial characteristics of reduced long-range functional connectivity in ASD. Compared to NT controls, ASD participants showed reduced alpha coherence between key anatomical components of a cognitive control network during preparation for a saccadic task. Moreover, unlike NT controls, they failed to modulate this coherence based on task demands. Reduced coherence and the failure to use context (here, the task cues) to modulate preparatory neural activity in accordance with task demands may contribute to impaired behavioral control in

ASD. These findings are consistent with the literature suggesting reduced cognitive control over behavior in ASD. They complement our recent fMRI report of reduced functional connectivity between the FEF and dACC during the same saccadic paradigm in the same participants (Agam et al., 2010), but add temporal and spectral specificity by demonstrating reduced coherence specifically during the preparatory period and in the alpha band.

ASD participants showed regionally specific reductions in alpha band coherence, which is the dominant rhythm associated with visuospatial attention (Busch et al., 2009; Ergenoglu et al., 2004; Hanslmayr et al., 2007; Mathewson et al., 2009). These findings are consistent with previous studies finding reduced alpha band coherence in ASD at rest using sensor space analysis (Murias et al., 2007; Tsiaras et al., 2011). In a review, Klimesch et al. (Klimesch et al., 2007) hypothesized that event-related synchronization in the alpha band plays an active role in top-down neural inhibitory control over cognitive performance. This hypothesis is relevant to our study because converging lines of evidence suggest that neural inhibition is abnormal in ASD. This evidence includes genetic studies implicating the γ-aminobutyric acid (GABA) receptor gene complex (Hussman, 2001; Ma et al., 2005), histological studies showing GABA receptor abnormalities (Blatt et al., 2001; Fatemi et al., 2009), and cortical minicolumns with reduced neuropil space (Casanova et al., 2003), which are a conduit for local inhibitory circuits. GABAergic neurons play a crucial role in saccade generation by the FEF. Local infusions of the GABA agonist muscimol into the FEF in rhesus monkeys interfered with the generation of saccades, while local injections of the antagonist bicuculine resulted in a large number of spontaneous saccades (Schiller and Tehovnik, 2003). Several other studies confirm that muscimol and other methods of deactivating the FEF interfere with saccades, and more so for tasks with increased cognitive requirements (Dias et al., 1995; Dias and Segraves, 1999; Keller et al., 2008). In humans, higher GABA levels in the FEF correlated with reduced susceptibility to visual distractors when making a saccade to a visual target (Sumner et al., 2010). In this context, we interpret the reduced and unmodulated alpha synchrony in the ASD group during preparation for a task requiring response inhibition as reflecting a failure in top-down cognitive control mechanisms that rely on neural inhibition.

The dACC emerged as the key cortical region showing connectivity with the FEF during saccadic preparation in both groups. This is consistent with its role in the top–down control of ocular motor regions, including the FEF (Johnston et al., 2007). The dACC shows greater activation for AS than PS (Brown et al., 2008; Doricchi et al., 1997; Ford et al., 2005; Manoach et al., 2007; Matsuda et al., 2004; Paus et al., 1993), which likely reflects the greater cognitive control required for AS, and lesions to the dACC increase the likelihood of AS errors (Milea et al., 2003). The posterior part of the dACC has been labeled the “cingulate eye field” because of its involvement in tasks requiring volitional, as opposed to reflexive, saccadic control (Gaymard et al., 1998; Paus et al., 1993; Pierrot-Deseilligny et al., 1995). Our findings of reduced and unmodulated coherence between the FEF and dACC are consistent with evidence of functional ACC abnormalities in ASD, including during response inhibition (Kana et al., 2007; Thakkar et al., 2008; Agam et al., 2010). Our findings are also consistent with evidence of structural abnormalities of the ACC in ASD, including reduced fractional anisotropy in the white matter underlying the dACC in our prior study that included the same participants (Thakkar et al., 2008) as well as other studies (Anderson et al., 2008; Barnea-Goraly et al., 2004; Ke et al., 2008; Ke et al., 2009). Finally, our hypothesis that the reduced alpha band synchrony we observed in the ASD subjects reflects a failure in inhibitory top-down control mechanisms is consistent with the finding that individuals with ASD have fewer $GABA_A$ receptors and benzodiazepine binding sites in the ACC (Oblak et al., 2009).

We note that our findings of reduced coherence of the FEF with the dACC in ASD were asymmetric and specific to either the inferior or superior FEF. Previous work has suggested that the right inferior (or lateral) FEF disproportionately contributes to the cognitive aspects of saccadic generation, while the left superior (or medial) FEF plays a more important role in motor planning (Petit et al., 2009). These relative specializations are consistent with our findings that the NT group modulated coherence with the FEFiR in accordance with task demands, while coherence with the FEFsL was similar across all conditions, which had identical motor requirements during the preparatory period (i.e., fixation). Furthermore, the coherence values between the FEFiR and the dACC were generally greater than those between the FEEFsL and the dACC. This observation supports a greater role for the right hemisphere and the right FEF in particular in spatial attention (McDowell et al., 2005). We caution, however, that these lateralized and regionally specific findings were not predicted, and may reflect the small sample size and consequent lack of power in the present study, which may also have led us to miss other meaningful effects.

Several other limitations of the present study merit consideration. Although ASD participants made almost twice as many antisaccade errors as controls (20 ±14% vs. 11 ±10 %), this difference was not significant. This result is discrepant with numerous prior reports of an increased antisaccade error rate in ASD, including our own slightly larger fMRI study (Thakkar et al., 2008) that included the participants of the present study. We attribute this discrepancy primarily to reduced power due to the small sample size. Another feature of the present study is that we provided a nickel bonus per correct response. This incentive was intended to elicit optimal performance by increasing attention and motivation, particularly in ASD participants who might be less motivated to perform well in response to the social demand characteristics of the experiment (e.g., they may be less motivated than NT controls to please the examiner by performing well). The literature on whether monetary rewards have differential effects on neural responses in ASD and NT individuals is mixed (Dichter et al., 2012; Larson et al., 2011; Schmitz et al., 2008). Unlike these prior studies of reward, however, in the present study there were no reward cues, there was no feedback on performance, the bonus amount was small and identical for all correct trials, and the bonus was remote in that it was added to the remuneration check that was mailed following study completion. Since all correct responses were rewarded equally regardless of trial type, in the comparisons of preparatory activation for different trial types any effect of the incentive should be minimal. Thus, our main finding that only healthy controls respond to antisaccades vs. prosaccades by increasing alpha coherence in a preparatory network, is difficult to explain in terms of a differential effect of the incentive across groups. The strong performance of both groups on the difficult antisaccade trials indicates that all participants were well-motivated and engaged in the task. Another limitation is that our sample was restricted to high functioning adults with ASD, and it is not clear whether our findings would generalize to younger or lower functioning participants. Finally, four ASD participants were taking medication at the time of the study (see Methods). Excluding those subjects was not an option due to the small sample size, but we note that our fMRI findings were similar when we excluded medicated participants (Agam et al., 2010), and inspection of individual data suggested that these subjects did not contribute disproportionately to the results.

5. Conclusions

In summary, we used MEG source localization techniques to examine the spectral and spatial characteristics of reduced functional connectivity between the anatomical components of a cognitive control network during a response inhibition task in ASD. Our findings complement our recent fMRI findings of reduced functional connectivity between the FEF and dACC during the same saccadic paradigm in the same participants (Agam et al.,

2010), but add temporal and spectral specificity by demonstrating reduced coherence specifically during the preparatory period, driven by reduced synchronization specifically in the alpha band. In accord with our prior fMRI findings, we also found that NT participants, but not ASD participants, increased alpha-mediated coherence in preparation for the more difficult AS task. Our interpretation of these findings is that inhibitory top-down control processes, mediated via alpha band synchronization, are impaired in ASD.

Supplementary Material

Refer to Web version on PubMed Central for supplementary material.

Acknowledgments

The authors would like to acknowledge grants from the Nancy Lurie Marks Family Foundation and from Autism Speaks (TK); NIMH (R01 MH67720 - DSM); Swedish Research Council, grant 2009-3765 (EVO); The National Center for Research Resources (P41RR14075, MSH), National Institute for Biomedical Imaging and Bioengineering (5R01EB009048, MSH), Cognitive Rhythms Collaborative: A Discovery Network (NFS 1042134, MSH), and Mental Illness Neuroscience Discovery (MIND) Institute (DOE DE-FG02-99ER62764, DSM).

Abbreviations

ASD	Autism Spectrum Disorder
NT	Neurotypical
AS	Antisaccades
PS	Prosaccades
FIX	Fixation
FEF	Frontal Eye Field
FEFsR/L	right and left superior FEF, respectively
FEFiR/L	right and left inferior FEF, respectively
dAAC	dorsal Anterior Cingulate Cortex
DLPFC	dorsolateral prefrontal cortex
MEG	Magnetoencephalography

Bibliography

Agam Y, Joseph RM, Barton JJ, Manoach DS. Reduced cognitive control of response inhibition by the anterior cingulate cortex in autism spectrum disorders. Neuroimage. 2010; 52:336–347. [PubMed: 20394829]

Anderson EJ, Husain M, Sumner P. Human intraparietal sulcus (IPS) and competition between exogenous and endogenous saccade plans. Neuroimage. 2008; 40:838–851. [PubMed: 18222708]

Barnea-Goraly N, Kwon H, Menon V, Eliez S, Lotspeich L, Reiss AL. White matter structure in autism: preliminary evidence from diffusion tensor imaging. Biol Psychiatry. 2004; 55:323–326. [PubMed: 14744477]

Belmonte MK, Allen G, Beckel-Mitchener A, Boulanger LM, Carper RA, Webb SJ. Autism and abnormal development of brain connectivity. J Neurosci. 2004; 24:9228–9231. [PubMed: 15496656]

Benjamini Y, Hochberg Y. Controlling the false discovery rate: a practical and powerful approach to multiple testing. Journal of the Royal Statistical Society Series B (Methodological). 1995; 57:289–300.

Blair JR, Spreen O. Predicting premorbid IQ: a revision of the National Adult Reading Test. Clin Neuropsychol. 1989; 3:129–136.

Blatt GJ, Fitzgerald CM, Guptill JT, Booker AB, Kemper TL, Bauman ML. Density and distribution of hippocampal neurotransmitter receptors in autism: an autoradiographic study. J Autism Dev Disord. 2001; 31:537–543. [PubMed: 11814263]

Bokil H, Purpura K, Schoffelen JM, Thomson D, Mitra P. Comparing spectra and coherences for groups of unequal size. J Neurosci Methods. 2007; 159:337–345. [PubMed: 16945422]

Brown MR, Vilis T, Everling S. Frontoparietal activation with preparation for antisaccades. J Neurophysiol. 2007; 98:1751–1762. [PubMed: 17596416]

Brown MR, Vilis T, Everling S. Isolation of saccade inhibition processes: rapid event-related fMRI of saccades and nogo trials. Neuroimage. 2008; 39:793–804. [PubMed: 17977025]

Busch NA, Dubois J, VanRullen R. The phase of ongoing EEG oscillations predicts visual perception. J Neurosci. 2009; 29:7869–7876. [PubMed: 19535598]

Capotosto P, Babiloni C, Romani GL, Corbetta M. Frontoparietal cortex controls spatial attention through modulation of anticipatory alpha rhythms. J Neurosci. 2009; 29:5863–5872. [PubMed: 19420253]

Casanova MF, Buxhoeveden D, Gomez J. Disruption in the inhibitory architecture of the cell minicolumn: implications for autism. Neuroscientist. 2003; 9:496–507. [PubMed: 14678582]

Coben R, Clarke AR, Hudspeth W, Barry RJ. EEG power and coherence in autistic spectrum disorder. Clin Neurophysiol. 2008; 119:1002–1009. [PubMed: 18331812]

Connolly JD, Goodale MA, Goltz HC, Munoz DP. fMRI activation in the human frontal eye field is correlated with saccadic reaction time. J Neurophysiol. 2005; 94:605–611. [PubMed: 15590732]

Connolly JD, Goodale MA, Menon RS, Munoz DP. Human fMRI evidence for the neural correlates of preparatory set. Nat Neurosci. 2002; 5:1345–1352. [PubMed: 12411958]

Dale AM, Fischl B, Sereno MI. Cortical surface-based analysis. I. Segmentation and surface reconstruction. Neuroimage. 1999; 9:179–194. [PubMed: 9931268]

Delorme A, Makeig S. EEGLAB: an open source toolbox for analysis of single-trial EEG dynamics including independent component analysis. J Neurosci Methods. 2004; 134:9–21. [PubMed: 15102499]

Dias EC, Kiesau M, Segraves MA. Acute activation and inactivation of macaque frontal eye field with GABA-related drugs. J Neurophysiol. 1995; 74:2744–2748. [PubMed: 8747229]

Dias EC, Segraves MA. Muscimol-induced inactivation of monkey frontal eye field: effects on visually and memory-guided saccades. J Neurophysiol. 1999; 81:2191–2214. [PubMed: 10322059]

Dichter GS, Felder JN, Green SR, Rittenberg AM, Sasson NJ, Bodfish JW. Reward circuitry function in autism spectrum disorders. Social cognitive and affective neuroscience. 2012; 7:160–172. [PubMed: 21148176]

Doricchi F, Perani D, Incoccia C, Grassi F, Cappa SF, Bettinardi V, Galati G, Pizzamiglio L, Fazio F. Neural control of fast-regular saccades and antisaccades: an investigation using positron emission tomography. Exp Brain Res. 1997; 116:50–62. [PubMed: 9305814]

Efron B. Size, power and false discovery rates. Ann Statist. 2007; 35:1351–1377.

Ergenoglu T, Demiralp T, Bayraktaroglu Z, Ergen M, Beydagi H, Uresin Y. Alpha rhythm of the EEG modulates visual detection performance in humans. Brain Res Cogn Brain Res. 2004; 20:376–383. [PubMed: 15268915]

Everling S, Munoz DP. Neuronal correlates for preparatory set associated with pro-saccades and anti-saccades in the primate frontal eye field. J Neurosci. 2000; 20:387–400. [PubMed: 10627615]

Fatemi SH, Reutiman TJ, Folsom TD, Thuras PD. GABA(A) receptor downregulation in brains of subjects with autism. J Autism Dev Disord. 2009; 39:223–230. [PubMed: 18821008]

First, MB.; Spitzer, RL.; Gibbon, M.; Williams, JBW. Biometrics Research. New York State Psychiatric Institute; New York: 2002. Structured Clinical Interview for DSM-IV-TR Axis I Disorders. Research Version, Nonpatient Edition

Fischer B, Breitmeyer B. Mechanisms of visual attention revealed by saccadic eye movements. Neuropsychologia. 1987; 25:73–83. [PubMed: 3574652]

Fischl B, Sereno MI, Dale AM. Cortical surface-based analysis. II: Inflation, flattening, and a surface-based coordinate system. Neuroimage. 1999a; 9:195–207. [PubMed: 9931269]

Fischl B, Sereno MI, Tootell RB, Dale AM. High-resolution intersubject averaging and a coordinate system for the cortical surface. Hum Brain Mapp. 1999b; 8:272–284. [PubMed: 10619420]

Ford KA, Goltz HC, Brown MR, Everling S. Neural processes associated with antisaccade task performance investigated with event-related FMRI. J Neurophysiol. 2005; 94:429–440. [PubMed: 15728770]

Gaymard B, Rivaud S, Cassarini JF, Dubard T, Rancurel G, Agid Y, Pierrot-Deseilligny C. Effects of anterior cingulate cortex lesions on ocular saccades in humans. Experimental brain research. Experimentelle Hirnforschung. Experimentation cerebrale. 1998; 120:173–183. [PubMed: 9629959]

Genovese CR, Lazar NA, Nichols T. Thresholding of statistical maps in functional neuroimaging using the false discovery rate. Neuroimage. 2002; 15:870–878. [PubMed: 11906227]

Ghuman AS, McDaniel JR, Martin A. A wavelet-based method for measuring the oscillatory dynamics of resting-state functional connectivity in MEG. Neuroimage. 2011; 56:69–77. [PubMed: 21256967]

Goldberg MC, Lasker AG, Zee DS, Garth E, Tien A, Landa RJ. Deficits in the initiation of eye movements in the absence of a visual target in adolescents with high functioning autism. Neuropsychologia. 2002; 40:2039–2049. [PubMed: 12208001]

Hämäläinen MS, Sarvas J. Feasibility of the homogeneous head model in the interpretation of neuromagnetic fields. Physics in medicine and biology. 1987; 32:91–97. [PubMed: 3823145]

Hamm JP, Dyckman KA, Ethridge LE, McDowell JE, Clementz BA. Preparatory activations across a distributed cortical network determine production of express saccades in humans. J Neurosci. 2010; 30:7350–7357. [PubMed: 20505102]

Hanslmayr S, Aslan A, Staudigl T, Klimesch W, Herrmann CS, Bauml KH. Prestimulus oscillations predict visual perception performance between and within subjects. Neuroimage. 2007; 37:1465–1473. [PubMed: 17706433]

Hollingshead, AB. Two factor index of social position. Yale University Press; New Haven, Conn: 1965.

Hussman JP. Suppressed GABAergic inhibition as a common factor in suspected etiologies of autism. J Autism Dev Disord. 2001; 31:247–248. [PubMed: 11450824]

Just MA, Cherkassky VL, Keller TA, Kana RK, Minshew NJ. Functional and anatomical cortical underconnectivity in autism: evidence from an FMRI study of an executive function task and corpus callosum morphometry. Cereb Cortex. 2007; 17:951–961. [PubMed: 16772313]

Kana R, Keller T, Minshew N, Just M. Inhibitory Control in High-Functioning Autism: Decreased Activation and Underconnectivity in Inhibition Networks. Biological Psychiatry. 2007; 62:198–206. [PubMed: 17137558]

Ke X, Hong S, Tang T, Zou B, Li H, Hang Y, Zhou Z, Ruan Z, Lu Z, Tao G, Liu Y. Voxel-based morphometry study on brain structure in children with high-functioning autism. Neuroreport. 2008; 19:921–925. [PubMed: 18520994]

Ke X, Tang T, Hong S, Hang Y, Zou B, Li H, Zhou Z, Ruan Z, Lu Z, Tao G, Liu Y. White matter impairments in autism, evidence from voxel-based morphometry and diffusion tensor imaging. Brain Res. 2009; 1265:171–177. [PubMed: 19233148]

Keller EL, Lee KM, Park SW, Hill JA. Effect of inactivation of the cortical frontal eye field on saccades generated in a choice response paradigm. J Neurophysiol. 2008; 100:2726–2737. [PubMed: 18784274]

Kleinhans NM, Richards T, Sterling L, Stegbauer KC, Mahurin R, Johnson LC, Greenson J, Dawson G, Aylward E. Abnormal functional connectivity in autism spectrum disorders during face processing. Brain. 2008; 131:1000–1012. [PubMed: 18234695]

Klimesch W, Sauseng P, Hanslmayr S. EEG alpha oscillations: The inhibition–timing hypothesis. Brain Research Reviews. 2007; 53:63–88. [PubMed: 16887192]

Koshino H, Kana RK, Keller TA, Cherkassky VL, Minshew NJ, Just MA. fMRI investigation of working memory for faces in autism: visual coding and underconnectivity with frontal areas. Cereb Cortex. 2008; 18:289–300. [PubMed: 17517680]

Koyama M, Hasegawa I, Osada T, Adachi Y, Nakahara K, Miyashita Y. Functional magnetic resonance imaging of macaque monkeys performing visually guided saccade tasks: comparison of cortical eye fields with humans. Neuron. 2004; 41:795–807. [PubMed: 15003178]

Larson MJ, South M, Krauskopf E, Clawson A, Crowley MJ. Feedback and reward processing in high-functioning autism. Psychiatry Research. 2011; 187:198–203. [PubMed: 21122921]

Lee AK, Hamalainen MS, Dyckman KA, Barton JJ, Manoach DS. Saccadic preparation in the frontal eye field is modulated by distinct trial history effects as revealed by magnetoencephalography. Cerebral Cortex. 2011; 21:245–253. [PubMed: 20522539]

Lin FH, Witzel T, Ahlfors SP, Stufflebeam SM, Belliveau JW, Hämäläinen MS. Assessing and improving the spatial accuracy in MEG source localization by depth-weighted minimum-norm estimates. Neuroimage. 2006; 31:160–171. [PubMed: 16520063]

Lord, C.; Rutter, M.; DiLavore, PC.; Risi, S. Autism Diagnostic Observation Schedule—WPS (ADOS-WPS). Western Psychological Services; Los Angeles, CA: 1999.

Luna B, Thulborn KR, Strojwas MH, McCurtain BJ, Berman RA, Genovese CR, Sweeney JA. Dorsal cortical regions subserving visually guided saccades in humans: an fMRI study. Cerebral Cortex. 1998; 8:40–47. [PubMed: 9510384]

Ma DQ, Whitehead PL, Menold MM, Martin ER, Ashley-Koch AE, Mei H, Ritchie MD, Delong GR, Abramson RK, Wright HH, Cuccaro ML, Hussman JP, Gilbert JR, Pericak-Vance MA. Identification of significant association and gene-gene interaction of GABA receptor subunit genes in autism. Am J Hum Genet. 2005; 77:377–388. [PubMed: 16080114]

Manoach DS, Lindgren KA, Barton JJ. Deficient saccadic inhibition in Asperger's disorder and the social-emotional processing disorder. Journal of neurology, neurosurgery, and psychiatry. 2004; 75:1719–1726.

Manoach DS, Thakkar KN, Cain MS, Polli FE, Edelman JA, Fischl B, Barton JJS. Neural Activity Is Modulated by Trial History: A Functional Magnetic Resonance Imaging Study of the Effects of a Previous Antisaccade. Journal of Neuroscience. 2007; 27:1791–1798. [PubMed: 17301186]

Mathewson KE, Gratton G, Fabiani M, Beck DM, Ro T. To see or not to see: prestimulus alpha phase predicts visual awareness. J Neurosci. 2009; 29:2725–2732. [PubMed: 19261866]

Matsuda T, Matsuura M, Ohkubo T, Ohkubo H, Matsushima E, Inoue K, Taira M, Kojima T. Functional MRI mapping of brain activation during visually guided saccades and antisaccades: cortical and subcortical networks. Psychiatry Research. 2004; 131:147–155. [PubMed: 15313521]

McDowell JE, Dyckman KA, Austin BP, Clementz BA. Neurophysiology and neuroanatomy of reflexive and volitional saccades: evidence from studies of humans. Brain Cogn. 2008; 68:255–270. [PubMed: 18835656]

McDowell JE, Kissler JM, Berg P, Dyckman KA, Gao Y, Rockstroh B, Clementz BA. Electroencephalography/magnetoencephalography study of cortical activities preceding prosaccades and antisaccades. Neuroreport. 2005; 16:663–668. [PubMed: 15858402]

Milea D, Lehericy S, Rivaud-Pechoux S, Duffau H, Lobel E, Capelle L, Marsault C, Berthoz A, Pierrot-Deseilligny C. Antisaccade deficit after anterior cingulate cortex resection. Neuroreport. 2003; 14:283–287. [PubMed: 12598747]

Minshew NJ, Luna B, Sweeney JA. Oculomotor evidence for neocortical systems but not cerebellar dysfunction in autism. Neurology. 1999; 52:917–922. [PubMed: 10102406]

Minshew NJ, Williams DL. The new neurobiology of autism: cortex, connectivity, and neuronal organization. Arch Neurol. 2007; 64:945–950. [PubMed: 17620483]

Moon SY, Barton JJS, Mikulski S, Polli FE, Cain MS, Vangel M, Hämäläinen MS, Manoach DS. Where left becomes right: A magnetoencephalographic study of sensorimotor transformation for antisaccades. Neuroimage. 2007; 36:1313–1323. [PubMed: 17537647]

Mosconi MW, Kay M, D'Cruz AM, Seidenfeld A, Guter S, Stanford LD, Sweeney JA. Impaired inhibitory control is associated with higher-order repetitive behaviors in autism spectrum disorders. Psychol Med. 2009; 39:1559–1566. [PubMed: 19154646]

Mostofsky SH, Powell SK, Simmonds DJ, Goldberg MC, Caffo B, Pekar JJ. Decreased connectivity and cerebellar activity in autism during motor task performance. Brain. 2009

Murias M, Webb S, Greenson J, Dawson G. Resting State Cortical Connectivity Reflected in EEG Coherence in Individuals With Autism. Biological Psychiatry. 2007; 62:270–273. [PubMed: 17336944]

Nagel M, Sprenger A, Lencer R, Kompf D, Siebner H, Heide W. Distributed representations of the "preparatory set" in the frontal oculomotor system: a TMS study. BMC Neurosci. 2008; 9:89. [PubMed: 18801205]

Oblak A, Gibbs TT, Blatt GJ. Decreased GABAA receptors and benzodiazepine binding sites in the anterior cingulate cortex in autism. Autism Res. 2009; 2:205–219. [PubMed: 19650112]

Oldfield RC. The assessment and analysis of handedness: the Edinburgh inventory. Neuropsychologia. 1971; 9:97–113. [PubMed: 5146491]

Paus T. Location and function of the human frontal eye-field: a selective review. Neuropsychologia. 1996; 34:475–483. [PubMed: 8736560]

Paus T, Petrides M, Evans AC, Meyer E. Role of the human anterior cingulate cortex in the control of oculomotor, manual, and speech responses: a positron emission tomography study. Journal of Neurophysiology. 1993; 70:453–469. [PubMed: 8410148]

Petit L, Zago L, Vigneau M, Andersson F, Crivello F, Mazoyer B, Mellet E, Tzourio-Mazoyer N. Functional Asymmetries Revealed in Visually Guided Saccades: An Fmri Study. J Neurophysiol. 2009

Pierrot-Deseilligny C, Rivaud S, Gaymard B, Müri R, Vermersch AI. Cortical Control of Saccades. Annals of Neurology. 1995; 37:557–567. [PubMed: 7755349]

Rutter L, Carver FW, Holroyd T, Nadar SR, Mitchell-Francis J, Apud J, Weinberger DR, Coppola R. Magnetoencephalographic gamma power reduction in patients with schizophrenia during resting condition. Human Brain Mapping. 2009; 30:3254–3264. [PubMed: 19288463]

Rutter, M.; Le Couteur, A.; Lord, C. Autism Diagnostic Interview—Revised. Western Psychological Services; Los Angeles, CA: 2003.

Schiller PH, Tehovnik EJ. Cortical inhibitory circuits in eye-movement generation. Eur J Neurosci. 2003; 18:3127–3133. [PubMed: 14656309]

Schmitz N, Rubia K, van Amelsvoort T, Daly E, Smith A, Murphy DG. Neural correlates of reward in autism. Br J Psychiatry. 2008; 192:19–24. [PubMed: 18174503]

Simo LS, Krisky CM, Sweeney JA. Functional neuroanatomy of anticipatory behavior: dissociation between sensory-driven and memory-driven systems. Cereb Cortex. 2005; 15:1982–1991. [PubMed: 15758195]

Straube A, Riedel M, Eggert T, Muller N. Internally and externally guided voluntary saccades in unmedicated and medicated schizophrenic patients. Part I. Saccadic velocity. Eur Arch Psychiatry Clin Neurosci. 1999; 249:1–6. [PubMed: 10195337]

Sumner P, Edden RA, Bompas A, Evans CJ, Singh KD. More GABA, less distraction: a neurochemical predictor of motor decision speed. Nat Neurosci. 2010; 13:825–827. [PubMed: 20512136]

Taulu S, Kajola M, Simola J. Suppression of interference and artifacts by the Signal Space Separation Method. Brain topography. 2004; 16:269–275. [PubMed: 15379226]

Taulu S, Simola J. Spatiotemporal signal space separation method for rejecting nearby interference in MEG measurements. Physics in medicine and biology. 2006; 51:1759–1768. [PubMed: 16552102]

Thakkar KN, Polli FE, Joseph RM, Tuch DS, Hadjikhani N, Barton JJ, Manoach DS. Response monitoring, repetitive behaviour and anterior cingulate abnormalities in autism spectrum disorders (ASD). Brain. 2008; 131:2464–2478. [PubMed: 18550622]

Tsiaras V, Simos PG, Rezaie R, Sheth BR, Garyfallidis E, Castillo EM, Papanicolaou AC. Extracting biomarkers of autism from MEG resting-state functional connectivity networks. Computers in biology and medicine. 2011

Uhlhaas P, Singer W. Neural Synchrony in Brain Disorders: Relevance for Cognitive Dysfunctions and Pathophysiology. Neuron. 2006; 52:155–168. [PubMed: 17015233]

Uhlhaas PJ, Haenschel C, Nikolic D, Singer W. The role of oscillations and synchrony in cortical networks and their putative relevance for the pathophysiology of schizophrenia. Schizophr Bull. 2008; 34:927–943. [PubMed: 18562344]

Uhlhaas PJ, Roux F, Rodriguez E, Rotarska-Jagiela A, Singer W. Neural synchrony and the development of cortical networks. Trends Cogn Sci. 2010

Uutela K, Taulu S, Hämäläinen M. Detecting and correcting for head movements in neuromagnetic measurements. Neuroimage. 2001; 14:1424–1431. [PubMed: 11707098]

Van Essen DC, Dierker DL. Surface-based and probabilistic atlases of primate cerebral cortex. Neuron. 2007; 56:209–225. [PubMed: 17964241]

White K, Ashton R. Handedness assessment inventory. Neuropsychologia. 1976; 14:261–264. [PubMed: 934460]

Highlights

- Spectral and spatial properties of coherence in ASD during saccades are examined.
- Alpha band long-range coherence between FEF and dACC was reduced in ASD.
- ASD subjects failed to modulate coherence with increasing task demands.
- Reduced alpha band synchrony may contribute to impaired behavioral control.

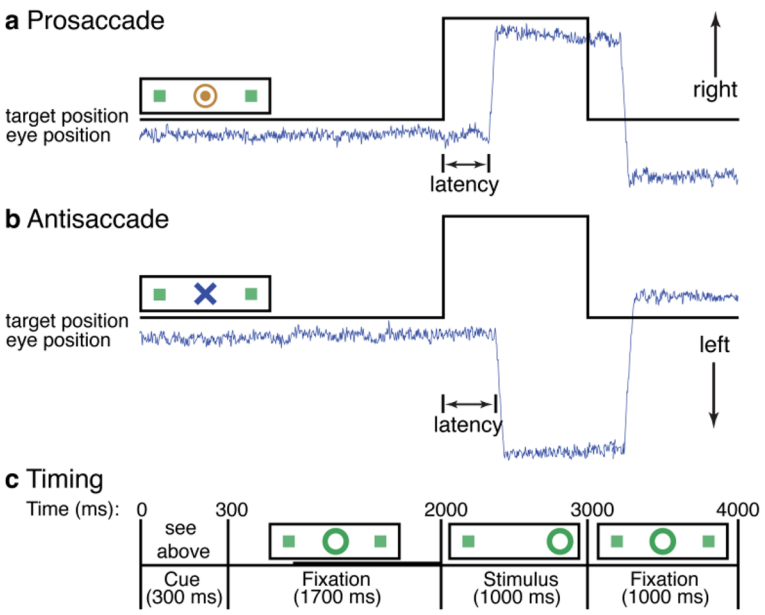

Figure 1.

Saccadic paradigm with idealized eye position traces. **(a,b)** Saccadic trials lasted 4 s and began with an instructional cue at the center of the screen. For half of the participants, orange concentric rings were the cue for a prosaccade trial (a) and a blue X was the cue for an antisaccade trial (b). These cues were reversed for the other half of the participants. The cue was flanked horizontally by two small green squares of 0.2° width that marked the potential locations of stimulus appearance, 10° left and right of center. These squares remained on the screen for the duration of each run. **(c)** After 300 ms, the instructional cue was replaced by a green fixation ring, of 0.4° diameter and luminance of 20 cd/m^2, at the center of the screen. 1700 ms later, the ring shifted to one of the two target locations, right or left, with equal probability. This was the stimulus to which the participant responded by making a saccade either to it (PS) or to the square on the opposite side (AS). The green ring remained in the peripheral location for 1000 ms and then returned to the center, where participants were to return their gaze for 1000 ms before the start of the next trial. Fixation intervals were simply a continuation of the fixation display that constituted the final second of the previous saccadic trial, and lasted 2 s, 4 s, or 6 s. The bold line in (c) indicates the time segment, 1000 ms preceding stimulus onset in saccade trials, used in our analyses.

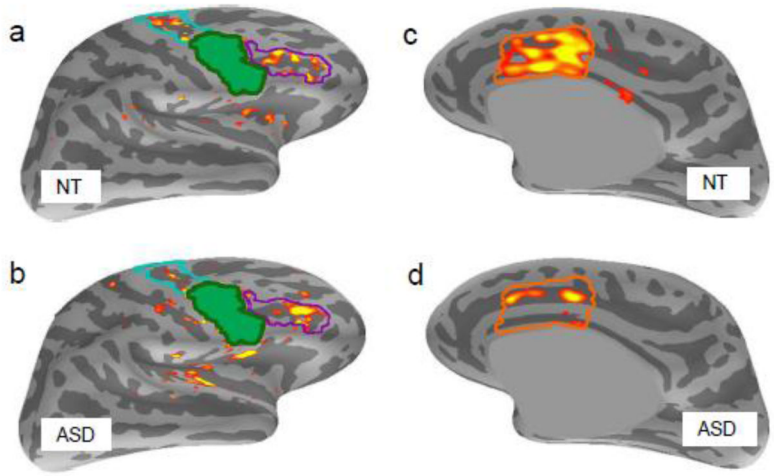

Figure 2.

Alpha-band coherence patterns in NT and ASD groups, during the AS condition. Colored vertices indicate significant coherence values with the FEFiR seed (in green) at a threshold of q<.1 on the inflated cortical surfaces. **(a)** Lateral cortical surface of the right hemisphere for controls and **(b)** ASD participants. The FEFsR is outlined in cyan, DLPFC in purple. **(c)** Medial cortical surface of the right hemisphere for NT participants, and **(d)** ASD participants. The FreeSurfer dACC label is outlined in orange.

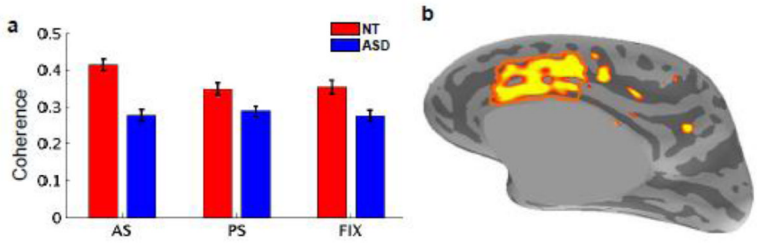

Figure 3.

Group by condition interaction for the FEFiR seed. **(a)** Bar graph of coherence between the FEFiR seed and the right dACC, averaged across all right dACC vertices, per condition, per group. Standard errors were computed using individual coherence values in the dACC across subjects, within each group. For each condition, coherence between the two regions was significantly reduced in the ASD group ($p<.00001$ for AS, $p<.01$ for PS/FIX). In the NT group coherence was significantly higher in the AS condition relative to the PS or FIX conditions ($p<.01$). Coherence was similar across all three conditions in the ASD group. **(b)** Result of the repeated measures ANOVA of coherence in cortical space showing a significant group by condition interaction in the right dACC (outlined in orange).

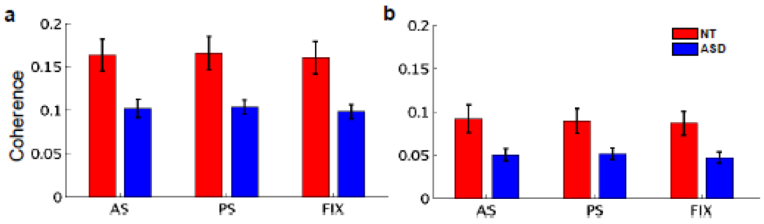

Figure 4.

Group differences in coherence with the FEFsL seed. Coherence between the FEFsL and **(a)** left and **(b)** right dACC, averaged across all vertices in the dACC label per hemisphere, per condition, per group. Standard errors were computed using individual coherence values in the dACC across subjects, within each group. No significant differences were observed across conditions in either group. The ASD group showed significantly reduced coherence between the FEFsL and the dACC in all conditions, in both the left ($p<.005$) and right ($p<.02$) hemispheres.

Table 1

Means and standard deviations for demographic data for each group. Two-tailed t-tests revealed no significant differences between groups.

Subject Characteristics	NT (n=11)	ASD (n=11)	p
Age	29 +/− 9	28 +/− 10	0.75
Sex	9M/2F	9M/2F	-
Estimated Verbal IQ	113 +/− 9	116 +/− 8	0.38
Parental SES	1.40 +/− 0.70	1.20 +/− 0.42	0.45
Years of Education	16 +/− 1	16 +/− 3	0.93
Laterality Score (handedness)	73 +/− 50	62 +/− 39	0.56